*Journal of Thermal Analysis and Calorimetry, Vol. 93 (2008) 3, 899–906*

# CALORIMETRIC STUDY OF ACTIVATED KINETICS OF THE NEMATIC AND SMECTIC PHASE TRANSITIONS IN AN ALIGNED NANO-COLLOIDAL LIQUID CRYSTAL+AEROSIL GEL

*D. Sharma*[*]

Department of Physics, Worcester Polytechnic Institute, Worcester, Massachusetts 01609, USA

This study explores the calorimetric analysis of an aligned nano-colloidal aerosil dispersed octyl-cyanobiphenyl gel. This system was prepared by solvent dispersion method (SDM). Heating scans were performed at different heating rates from 20 to 1 K $min^{-1}$ using DSC. Aligned samples follow Arrhenius behavior and showed a temperature shift in SmA–N and N–I transitions towards lower temperature. These samples show a decreased activated kinetics and an interesting relationship with their enthalpy. This behavior can be explained in terms of surface and molecular interaction between aerosil nano-particles and 8CB molecules and produced strain in the system.

***Keywords:*** calorimeter, nano-colloids, orientational order of liquid crystal, surface dynamics

## Introduction

Liquid crystals in its pure form are materials for fundamental research and technical application because of their specific molecular alignment [1–3], whereas the presence of tiny particles like aerogels or aerosil nano-particles creates a disorder and changes the order and alignment of the molecule of liquid crystals [4, 5]. The hydrophilic nature of the aerosils allow the silica particles to weakly hydrogen bond to each other and form a gel in an organic solvent which changes the thermodynamics as well as the alignment of the system and increases the scientific interest to study these types of systems [5–7].

Aerosil dispersed octylcyanobiphenyl (8CB), has been studied by various authors to understand smectic-A to nematic (SmA–N) and nematic to isotropic (N–I) transitions using light scattering, X-ray diffraction and AC calorimetry [6, 8–10], where AC calorimetry focused on phase change and specific heat capacity of the phase transitions of such systems [6, 11]. It would be interesting to study nano-colloidal aerosil dispersed liquid crystal systems under the effect of magnetic field to understand the kinetics of the phase transitions. No report has been found on activated kinetics of the phase transitions of such systems under the effect of magnetic field. Only a few studies report the effect of magnetic field on aerosil dispersed liquid crystals using optical and rheological technique but do not focus on kinetics and thermodynamics of the system [12–16]. Therefore, we report a detailed calorimetric study to understand the activated kinetics of SmA–N and N–I phase transitions for magnetized or aligned nano-colloidal aerosil dispersed 8CB liquid crystal system using Arrhenius theory. Calorimetry technique is a good tool to study thermal, phase and rate kinetics of various research and scientific materials for long time [7, 17–21]. The activated kinetics of such systems in the absence of magnetic field was described in our recent published work [11, 22, 23].

Hence, this study reports the kinetics of SmA–N and N–I phase transitions of three different densities of aerosils in 8CB liquid crystal under the effect of magnetic field using Arrhenius theory. Heating scans were performed using DSC at four different ramp rates for all samples. Sample details and experimental procedure are described in 'Experimental'. The results with the required theory are shown in 'Results', with discussion and conclusions drawn in 'Discussions' and 'Conclusions'.

## Experimental

### *Nano-colloidal system*

The nano-colloidal system, used in this study, was the mixture of hydrophilic type-300 aerosil nano-particles in the bulk octylcyanobiphenyl 8CB liquid crystal that forms a gel. The diameter of aerosil nano-particles is roughly 7 nm whereas the length of 8CB molecules is 2 nm and the width is 0.5 nm and the specific surface area of type-300 aerosil nano-particle is 300 $m^2$ $g^{-1}$,

* dr_dipti_sharma@yahoo.com

*1388–6150/$20.00*

*Akadémiai Kiadó, Budapest, Hungary*
*Springer, Dordrecht, The Netherlands*

[24]. The molecular mass of bulk 8CB and aerosil nano-particles ($SiO_2$) are $M_w$=291.44 g mol$^{-1}$ and $M_w$=60.08 g mol$^{-1}$, respectively. The bulk 8*CB* was obtained from Frinton Laboratories and aerosil nano-particles were obtained from Degussa. This nano-colloidal mixture was prepared by solvent dispersion method (SDM). The detailed procedure of this method can be seen in these publications. [6, 22, 23]. In the system, the density of the aerosil nano-particles in the bulk of 8CB was varied in three steps from 0.05, 0.10 and 0.20 g cm$^{-3}$. These samples were degassed for about 1 h under a vacuum unit at room temperature 293 K and then used for magnetization.

First, these samples were sealed into the aluminium cells and then they were placed into the magnetic field to get aligned. During the magnetization, the cycling of the samples were done in between smectic A and isotropic phases in the presence of a magnetic field of 0.5 T. The temperature range of this cycling was 300 to 318 K. The number of cycling was 10. After treating sample under magnetic field, the samples underwent the calorimetric measurements to DSC with the unaligned samples from the same batch as the aligned ones. Freshly aligned samples were used in DSC for each run. The calorimetric measurements follow the method described below.

*Methods*

The nano-colloidal 8CB system was studied by differential scanning calorimetry (DSC) using a model MDSC 2920 (TA instruments). Rate dependent heating scans were performed for all aligned and unaligned samples where heating ramp rates were varied from 20 to 1 K min$^{-1}$ rates. Three different densities of aerosil nano-particles were studied in bulk 8CB. The lowest density (0.05 g cm$^{-3}$ with sample mass 2.5 mg) was heated from 243 to 333 K at 20 K min$^{-1}$ ramp rate. The respective heat flow of the sample was recorded along with temperature change during heating scans. Similar measurements were made at heating scan rates of 10, 5 and 1 K min$^{-1}$ with fresh aligned samples. Experimental and environmental conditions were kept identical for all runs so that a comparison of the phase transition parameters could be made to understand the effect of different heating rates on phase transitions of the sample. The above steps were repeated for other densities of aerosol nano-particles (0.10 and 0.20 g cm$^{-3}$) using the same procedure. Each time fresh aligned sample was used. The complete procedure was repeated several times with the same and fresh aligned samples to confirm the accuracy of results. These results were compared with the results of unaligned samples. The temperatures of endothermic peaks are reported at the maximum height of peaks instead of the onset temperature because the temperature at peak maxima reflects the maximum change in the enthalpy.

## Results and discussion

*Effect of heating scan on alignment*

Figure 1 shows a comparative heating scan of aligned and unaligned sample of 0.5 g cm$^{-3}$ at 5 K min$^{-1}$ heating ramp rate spanning the isotropic and smectic phases. Aligned sample shows a temperature shift to-

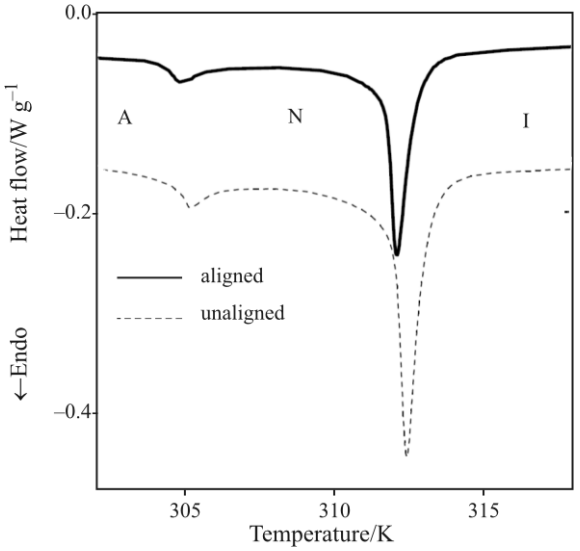


**Fig. 1** Heat flow *vs.* temperature at 5 K min$^{-1}$ heating ramp rate for the aligned and unaligned 8CB+Sil density 0.05 g cm$^{-3}$. The region A, N and I represents smectic A, nematic and isotropic state of the system respectively

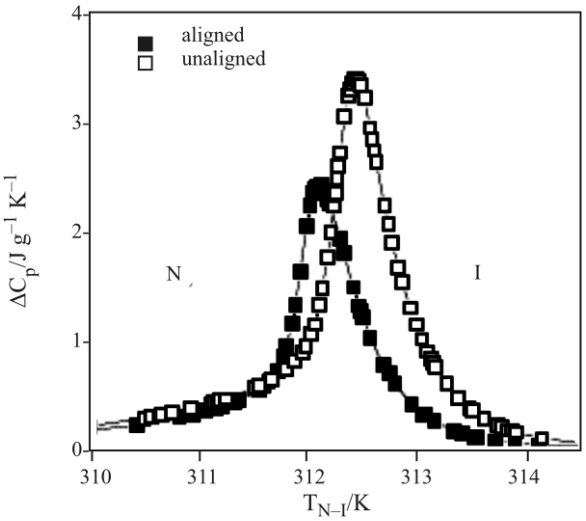


**Fig. 2** The excess of specific heat capacity *vs.* temperature for N–I transition of the aligned and unaligned samples for the same density at the same ramp rate

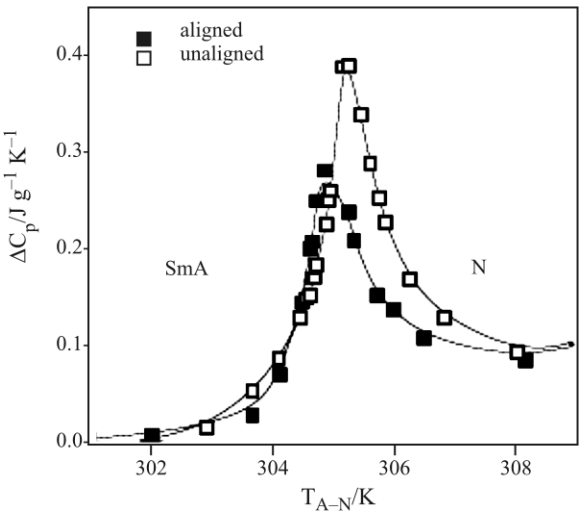


**Fig. 3** The excess of specific heat capacity *vs.* temperature for the SmA–N transition of the aligned and unaligned samples for the same density at the same ramp rate

wards lower temperature for SmA–N and N–I transitions having smaller peak size when compared to the unaligned sample. To see clear effect of alignment, the excess of specific heat capacity of N–I and SmA–N transitions are plotted in Figs 2 and 3, respectively. It is clear that the first order transition N–I shows maximum shift as well as maximum change in its enthalpy when compared with the second order transition SmA–N for aligned samples.

*Effect of ramp rates on alignment*

Rate dependent study of the aligned system was performed at different heating ramp rates of 20, 10, 5 and 1 K min$^{-1}$. It showed significant shifts in peak temperature following an Arrhenius behavior. This shift decreases for the aligned samples when compared with the unaligned samples. To see clear shifts in each transition, the excess of specific heat capacity was plotted for each transition. The excess specific heat capacity for the system was obtained by subtracting from the specific heat $C_p$ a linear background as

$$\Delta C_p = C_p - C_p\,(\text{background}) \qquad (1)$$

where $C_p$(background) is the baseline and $C_p$ is the specific heat capacity of the sample. Figure 4 shows a comparative plot of aligned and unaligned sample of lowest density as the excess of specific heat capacity of N–I transition. As ramp rate decreases transition peak shifts towards lower temperature following an Arrhenius behavior. Aligned samples show a decreased shift with having broader and smaller peaks, whereas SmA–N transition shows smallest peaks with wings as shown in Fig. 5 for the same density. The specific heat contribution of the SmA–N transition is

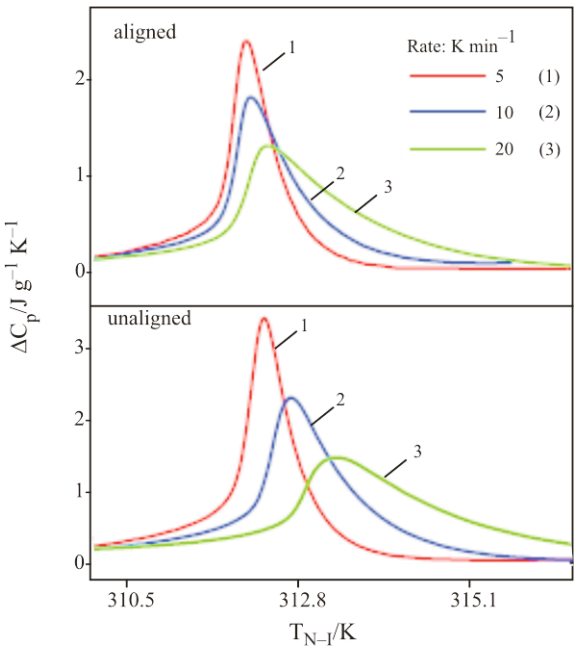


**Fig. 4** Comparison of $\Delta C_p$ between aligned and unaligned heating rate effect for N–I transition for 0.05 g cm$^{-3}$ density varying ramp rates from 20 to 5 K min$^{-1}$

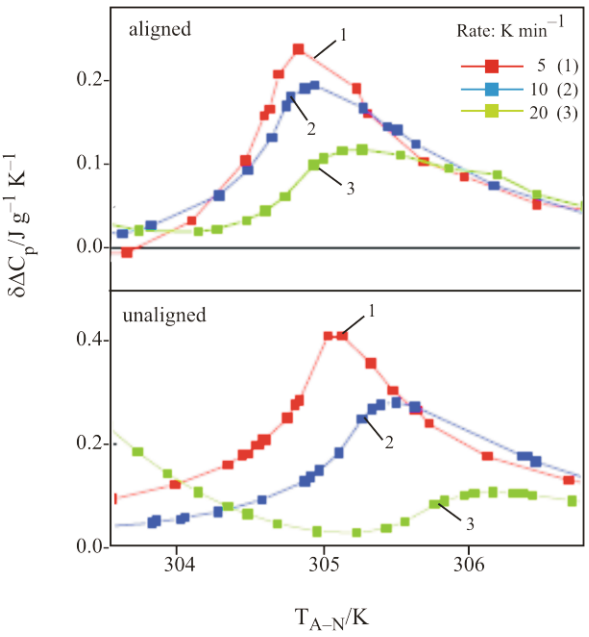


**Fig. 5** Comparison of $\Delta C_p$ between aligned and unaligned heating rate effect for SmA–N transition for 0.05 g cm$^{-3}$ density varying ramp rates from 20 to 5 K min$^{-1}$

obtained from $\Delta C_p$ by subtracting the heat capacity wing of the N–SmA transition

$$\delta C_p = \Delta C_p - \Delta C_p^{\text{wing}}\,(\text{NA}) \qquad (2)$$

It is clear from Fig. 5 that the SmA–N transition follows Arrhenius behavior and shifts towards lower temperature as ramp rate decreases. The shifting rate

and peak size is minimum for SmA–N transition than N–I transition for aligned samples. The Arrhenius behavior found in peak shifting indicates activation energy for each transition.

Similar rate effects were also found for 0.10 and 0.20 g cm$^{-3}$ densities of aerosil nano-particles, but for simplicity, these plots are not shown here. These results were considered in the data analysis. Transitions follow an Arrhenius behavior with different heating ramp rates and show rate dependent thermal dynamics.

*Arrhenius behavior*

According to Arrhenius theory [25–28], the effective heating rate can be given by

$$\beta=\beta_0\left[\exp\left(\frac{-\Delta E}{RT}\right)\right] \quad (3)$$

where β is the effective heating rate in K min$^{-1}$, $\beta_0$ is a constant in K min$^{-1}$, $\Delta E$ is the activation energy in J mol$^{-1}$, $R$ is the universal gas constant in J mol$^{-1}$ and $T$ is the absolute temperature in K. This equation can also be shown as

$$\ln\beta=\ln\beta_0-\left(\frac{\Delta E}{RT}\right) \quad (4)$$

where $\Delta E$ is determined from the slope of the graph, which is plotted between lnβ and 1 T$^{-1}$.

Figure 6 shows a comparative Arrhenius plot for aligned and unaligned samples for N–I transition and Fig. 7 shows SmA–N transition. Aligned samples follow Arrhenius behavior and indicate a changed activated kinetics for the phase transitions. Aligned samples show wider range of variation in the activation energy for both transitions when compared with the unaligned. Aligned samples show an increase in the activation energy for both phase transitions at the lowest density of aerosils 0.05 g cm$^{-3}$. As aerosil density increases further, activation energy decreases for 0.10 g cm$^{-3}$ and then increases for the further increase of aerosil density. Second order phase transition SmA–N has greater activation energy than N–I transition. The values of activation energy for both phase transitions of aligned samples are shown in Table 1.

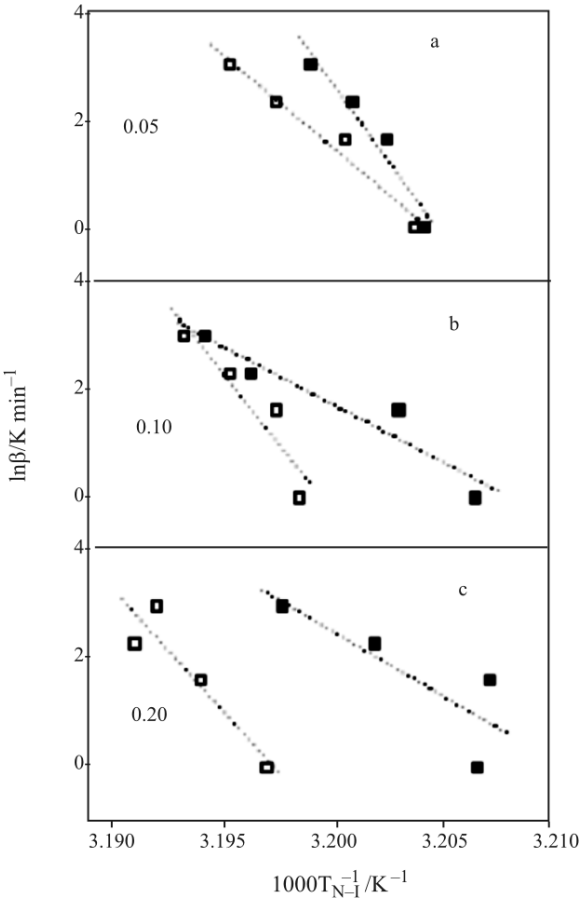


**Fig. 6** Arrhenius plot to compare the aligned and unaligned samples for N–I transition; a – 0.05, b – 0.10 and c – 0.20 g cm$^{-3}$ densities. Closed and open symbols represent aligned and unaligned samples. The dotted lines are the fits to the data points

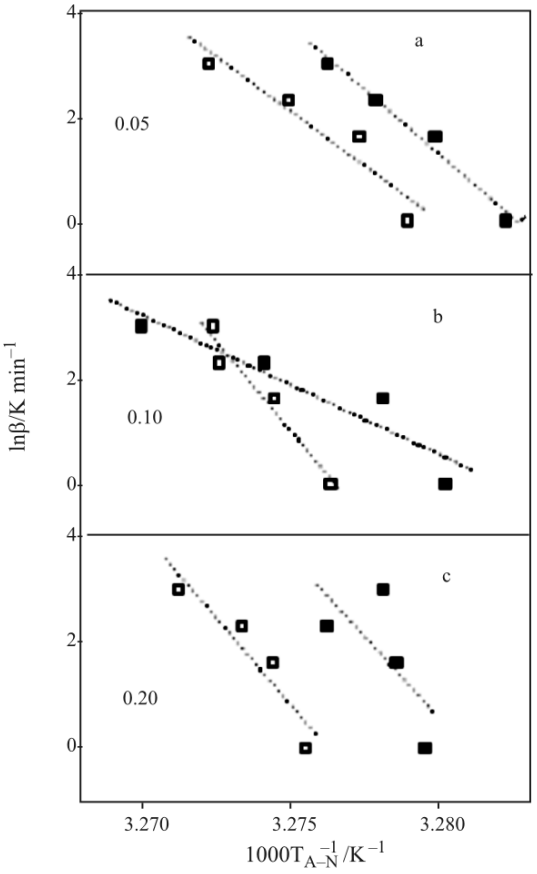


**Fig. 7** Arrhenius plot to compare the aligned and unaligned samples for SmA–N transition; a – 0.05, b – 0.10 and c – 0.20 g cm$^{-3}$ densities. Closed and open symbols represent aligned and unaligned samples. The dotted lines are the fits to the data points

**Table 1** Data details for aligned system; enthalpy, activation energy and entropy with aerosol density variation. Shown are the density of aerosil nano-particles density, enthalpy, activation energy and entropy for A–N and and N–I transitions

| Density, ρ/ g cm$^{-3}$ | $\Delta H_{A-N}$/ kJ mol$^{-1}$ | $\Delta H_{N-I}$/ kJ mol$^{-1}$ | $\Delta E_{A-N}$/ kJ mol$^{-1}$ | $\Delta E_{N-I}$/ kJ mol$^{-1}$ | $\Delta S_{A-N}$/ J mol$^{-1}$ K$^{-1}$ | $\Delta S_{N-I}$/ J mol$^{-1}$ K$^{-1}$ |
|---|---|---|---|---|---|---|
| 0.05 | 0.09 | 1.07 | 5.04 | 4.82 | 0.32 | 3.41 |
| 0.10 | 0.15 | 1.57 | 1.92 | 1.82 | 0.50 | 5.02 |
| 0.20 | 0.10 | 1.47 | 5.10 | 1.94 | 0.31 | 4.70 |

*Effect of nano-colloidal density on alignment*

As aerosil density increases in the system, both transition peaks shift towards lower, a little higher and then lower temperatures and transition peaks become smaller and broader for aligned samples, as shown in Figs 8 and 9. Variation in peak position for both transitions as a function of aerosil density can be seen in Fig. 10. It is clear from this figure that the range of variation of peak positions decreases for aligned samples. Due to the decreased change in peak position of both transitions, the temperature range between SmA–N and N–I transitions also decreases, as shown in Fig. 11.

The peak positions were calculated, in Fig. 10 for all densities as $\Delta T(K)=T(\rho_s)-T^0$, where $T(\rho_s)$ represents the peak temperature of various transitions for different densities and $T^0$ represents for bulk 8CB for the aligned and unaligned samples. Furthermore, the temperature range between SmA–N and N–I transitions were calculated, in Fig. 11 for all densities as $\Delta T_{AN}(K)=T_{N-I}(\rho_s)-T_{A-N}(\rho_s)$ where $T(\rho_s)$ represents the peak temperature of the transitions for different densities.

Enthalpy of each phase transition changes with the aerosil density and follows a pattern of variation. Aligned sample shows a decrease in enthalpy at 0.05 g cm$^{-3}$ density of aerosil and then increases for

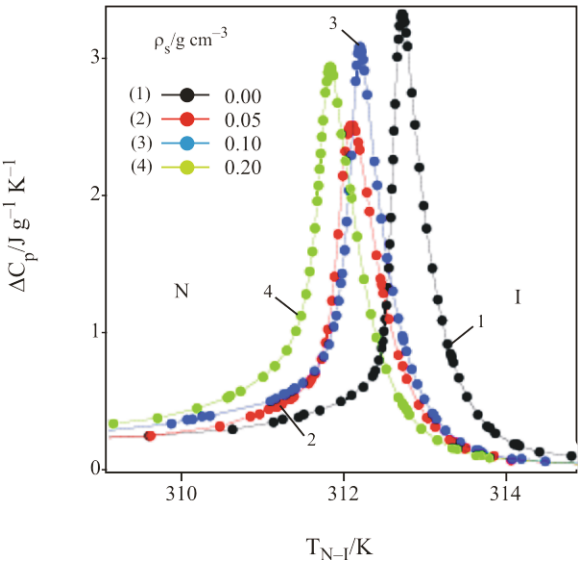


**Fig. 8** The excess of specific heat capacity *vs.* temperature of aligned samples for all densities of aerosils to show N–I transition at 5 K min$^{-1}$ heating ramp rate

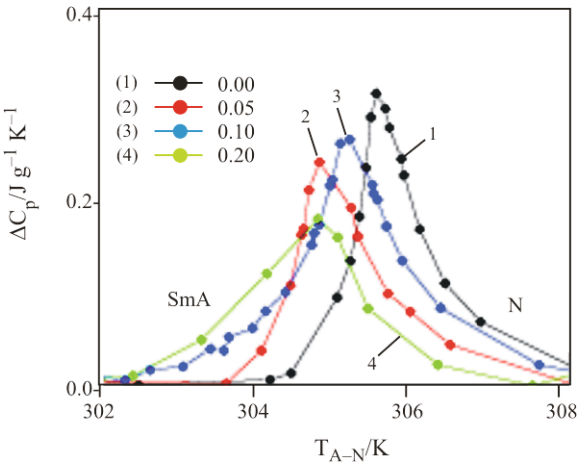


**Fig. 9** The excess of specific heat capacity *vs.* temperature of aligned samples to show SmA–N transition for all densities at 5 K min$^{-1}$ heating ramp rate

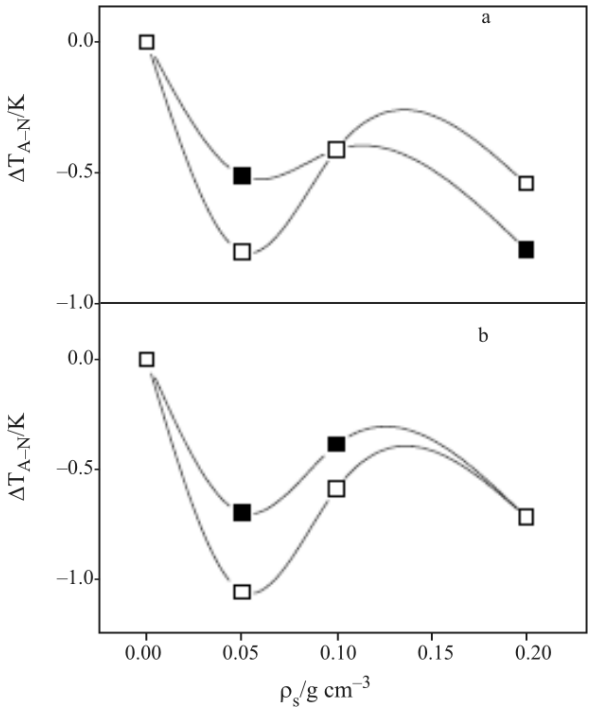


**Fig. 10** The effect of magnetic field on the peak positions of each transition; a – N–I and b – SmA–N transitions at 5 K min$^{-1}$ ramp rate. Closed and open symbols represent aligned and unaligned samples

**Table 2** Data details for unaligned system: enthalpy, activation energy and entropy

| Density, ρ/ g cm$^{-3}$ | $\Delta H_{A-N}$/ kJ mol$^{-1}$ | $\Delta H_{N-I}$/ kJ mol$^{-1}$ | $\Delta E_{A-N}$/ kJ mol$^{-1}$ | $\Delta E_{N-I}$/ kJ mol$^{-1}$ | $\Delta S_{A-N}$/ J mol$^{-1}$ K$^{-1}$ | $\Delta S_{N-I}$/ J mol$^{-1}$ K$^{-1}$ |
|---|---|---|---|---|---|---|
| 0.05 | 0.14 | 1.37 | 4.29 | 2.92 | 0.46 | 4.41 |
| 0.10 | 0.10 | 1.17 | 4.93 | 3.66 | 0.33 | 3.76 |
| 0.20 | 0.07 | 0.97 | 5.41 | 4.38 | 0.24 | 3.13 |

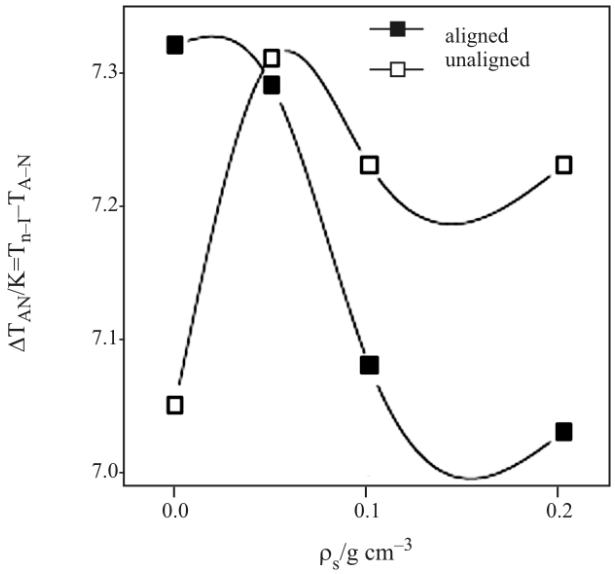


**Fig. 11** The effect of magnetic field on the temperature range between SmA–N and N–I transitions at 5 K min$^{-1}$ ramp rate

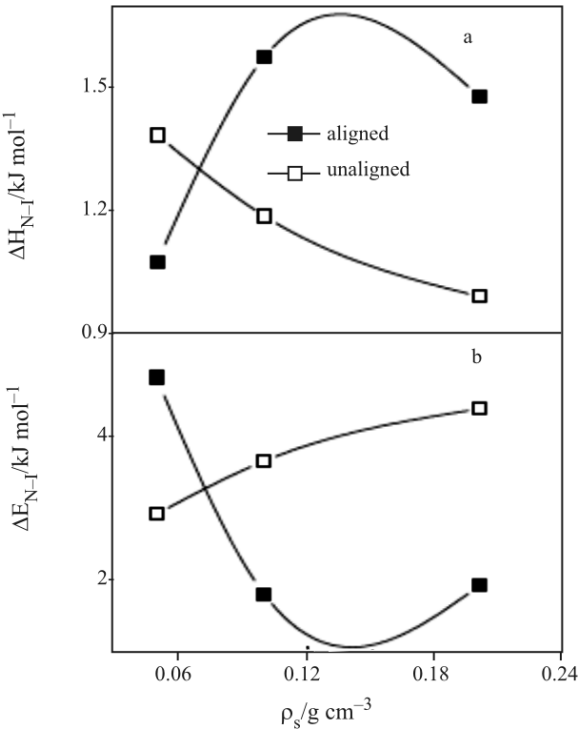


**Fig. 12** Comparison between enthalpy and activation energy of aligned and unaligned samples for N–I transition; a – change in the enthalpy and b – change in the activation energy

further increase of aerosil up to 0.10 g cm$^{-3}$ and then decreases for the highest density 0.20 g cm$^{-3}$, whereas, unaligned sample shows a decrease in their enthalpy with the increase of aerosil density. First order transition N–I has larger enthalpy variation than second order transition. Enthalpy variation can be seen in Tables 1 and 2 for the aligned and unaligned samples respectively.

Rate dependent calorimetric study of aligned aerosil dispersed 8CB system brings interesting changes in the thermodynamics of the phase transitions. The presence of magnetic field in the system changes the activated kinetics of the transition. This kinetics shows an interesting relationship between activation energy and enthalpy of the phase transition. This kinetics can be studied using Arrhenius theory which represents the energy of the ordered-disordered molecular motion and rearrangement of each transition near the transition temperature [25–28].

Figures 12 and 13 show a comparative plot between enthalpy and activation energy for the N–I and SmA–N transitions for aligned and unaligned samples respectively. As aerosol density increases in the aligned system, the enthalpy decreases at 0.05 g cm$^{-3}$ density of aerosil and then increases and becomes maximum for 0.10 and then decreases for the further increase of aerosils and becomes minimum for 0.20 g cm$^{-3}$, whereas the respective activation energy of the transition decreases and becomes minimum for 0.10 and then increases and becomes maximum for 0.20 g cm$^{-3}$ for aligned samples. It is clear that enthalpy and activation energy follow a pattern of variation in reverse direction and indicates that enthalpy and activation energy of the phase transitions are reversely proportional. Enthalpy is the energy absorbed during the transition (in terms of endothermic peak) and activation energy is the required energy for the transition. Hence, enthalpy and activation relationship follows that if the transition absorbs more energy, it will require less energy. Unaligned samples also follow this relationship but show a continuous decrease in enthalpy and increase in activation energy as aerosil density increases. The effect of magnetic field brings maximum change in the system at 0.10 g cm$^{-3}$ density of aerosil and indicates maximum dynamics at this point. This can be explained as follows.

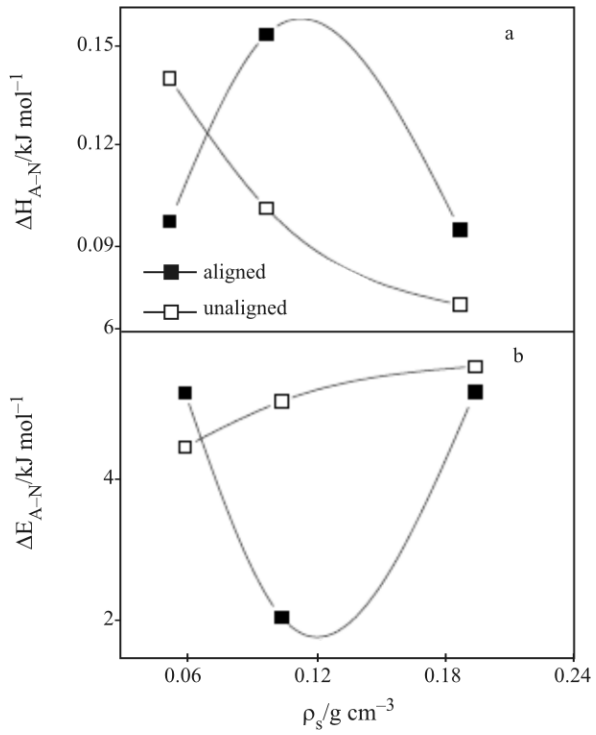


**Fig. 13** Comparison between enthalpy and activation energy of aligned and unaligned samples for SmA–N transition; a – change in the enthalpy and b – change in the activation energy

The 8CB liquid crystal is a well-studied proto-typical rod-like molecule, with a rigid biphenyl core at one end attached to an aliphatic tail and other to a polar cyano group. Whereas, the aerosil nano-particles consists of $SiO_2$ (silica) spheres is coated with (–OH) hydroxyl groups exposed on the surface. The hydroxy groups on the surface, enable the spheres to hydrogen bond and form a thixotropic fractal gel in an organic medium, such as 8CB and changes the thermodynamics of the system [29, 30]. The mutual interaction between aerosil nano-particles and liquid crystal molecules increases due to the formation of hydrogen bonds as aerosil density increases. It becomes maximum for 0.10 g cm$^{-3}$ density of aerosils and starts decreasing as density increases further. As density further increases above 0.10 g cm$^{-3}$, the self-interaction between aerosil nano-particles increases due to formation of Si–O–Si bonds and increases more disorder in the system and shows a decrease in dynamics [22]. In the aligned samples, due to the presence of magnetic force, liquid crystal molecules get more aligned and more ordered. This creates a strain in the system and makes molecules more bound [16]. For the lowest density of aerosil 0.05 g cm$^{-3}$, system feels less strain and absorbs less energy to go through the transition and shows a decrease in enthalpy and needs more activation energy. For further increase of aerosil density, as density increases, strain in the system increases and hence system absorbs more energy and shows an increase in enthalpy and decrease in activation energy. But for the highest density, self-interaction between aerosil particles reaches maximum, due to which strain in the system decreases and hence shows a decrease in enthalpy and increase in activation energy. Second order transition SmA–N has smaller enthalpy with no latent heat than first order N–I transition, hence, SmA–N transition shows higher activation energy than first order transition. Data details for the aligned and unaligned samples are given in the Tables 1 and 2, respectively.

## Conclusions

The study of activated kinetics of SmA–N and N–I transitions of aligned aerosil nano-particle dispersed 8CB system has been done by performing heating rate dependent experiments using DSC. The transition peak temperature for SmA–N and N–I phase transitions as well as the temperature range between these two-phase transitions decrease. The activation energy of the aligned system increases and its respective enthalpy decreases for the lowest density of aerosils 0.05 g cm$^{-3}$, but for the further increase of aerosil density, the activation energy decreases and its respective enthalpy increases for both phase transitions.

Overall, aligned samples show a decreased activated kinetics as aerosil density increases in the system, where the second order transition SmA–N has higher activation than weak first order N–I transition. This can be explained in terms of molecular interaction and developed strain in between aerosil nano-particles and liquid crystal molecules in the aligned system. As aerosil nano-particles are added into bulk 8CB, a surface interaction takes place between molecules where aerosil particles are found to be coated with 8CB molecules and interact with each other under a weak hydrogen bond interaction. As density of aerosil nano-particles increases in the system, mutual interaction increases and becomes maximum for 0.10 density of aerosil in the system; and hence shows maximum change for this density. As density further increases, the self-interaction between aerosil nano-particles increases due to formation of Si–O–Si bonds and increases more disorder in the system [23]. For the aligned samples, due to the effect of magnetic force, the alignment of liquid crystals changes. They get more aligned due to which system experiences a strain and hence interaction between aerosil nano-particles and liquid crystal molecules decreases. This indicates a decrease in the activated kinetics of the aligned system. The second order transition SmA–N has smaller enthalpy with no latent heat

which represents smaller enthalpy and hence it needs more and higher activation than weak first order N–I transition. This indicates a decrease in the activated kinetics of the aligned system.

## Acknowledgements

The author is grateful to G. S. Iannacchione for many useful discussions and J. C. Mac-Donald for DSC instrument.

## References

1 T. Shima, M. Okumura and T. Higuchi, Electronics and Communications in Japan, Part 2 (Electronics), 79 (1996) 73.
2 H. Cheng and H. Gao, J. Appl. Phys., 87 (2000) 7476.
3 C. C. Yu and H. M. Carruzzo, Phys. Rev. E, 69 (2004) 051201.
4 N. P. da Silveira, F. E. Dolle, C. Rochas, A. Rigacci, F. V. Pereira and H. Westfahl Jr., J. Therm. Anal. Cal., 79 (2005) 579.
5 T. Bellini, N. A. Clark, V. Degiorgio, F. Mantegazza and G. Natale, Phys. Rev. E, 57 (1998) 2996.
6 G. S. Iannacchione, C. W. Garland, J. T. Mang and T. P. Rieker, Phys. Rev. E, 58 (1998) 5966.
7 D. Sharma and G. S. Iannacchione, J. Chem. Phys, 126 (2007) 094503.
8 R. L. Leheny, S. Park, R. J. Birgeneau, J. L. Gallani, C. W. Garland and G. S. Iannacchione, Phys. Rev. E, 67 (2003) 011708.
9 T. Jin and D. Finotello, Phys. Rev. Lett., 86 (2001) 818.
10 R. Nozaki, T. K. Bose and S. Yagihara, Phys. Rev. A, 46 (1992) 7733.
11 D. Sharma, J. C. MacDonald and G. S. Iannacchione, J. Phys. Chem. B, 110 (2006) 16679.
12 A. D. Bagmet and A. L. Tsykalo, J. Eng. Phys., 52 (1987) 279.
13 F. Li, W. J. Doane and A. J. Kli, Japanese J. Appl. Phys., 45 (2006) 1714.
14 P. G. de Gennes and J. Prost, The Physics of Liquid Crystals, 2nd Ed., Clarendon Press, Oxford, England 1993.
15 E. Lizuka, Inter. J. Polym. Mater., 45 (2000) 191.
16 D. Liang, M. A. Borthwick and R. L. Leheny, J. Phys. Condens. Matter., 16 (2004) S1989.
17 C. R. Ernst, G. M. Schneider, A. W. Rflinger and W. Weiflog, Ber. Bunsenges. Phys. Chem., 102 (1998) 1870.
18 D. Sharma, R. Shukla, A. Singh, A. Nagpal and A. Kumar, Adv. Mater. Opt. Electron., 10 (2000) 251.
19 D. Sharma, S. K. Dwivedi, R. K. Shukla and A. Kumar, Mater. Manufact. Proc., 18 (2003) 93.
20 D. Sharma, R. Shukla and A. Kumar, Thin Solid Films, 357 (1999) 214.
21 N. Mehta, D. Sharma and A. Kumar, Physica B, 391 (2007) 108112.
22 D. Sharma, J. C. MacDonald and G. S. Iannacchione, J. Phys. Chem. B, 110 (2006) 26160.
23 D. Sharma and G. S. Iannacchione, J. Phys. Chem. B, 111 (Mar 2007) 1916.
24 Degussa Corp., Silica Division, 65 Challenger Road, Ridgefield Park, NJ 07660. Technical data is given in the Degussa booklet Aerosila.
25 H. Vogel, Phys. Z., 22 (1921) 645.
26 G. S. Fulcher, J. Am. Ceram. Soc., 6 (1926) 339.
27 D. Maximean, C. Rosu, T. Yamamoto and H. Yokoyama, Molecular Crystals Liquid Crystals, 417 (2004) 215.
28 F. Blum, A. Padmanabhan and R. Mohebbi, Langmuir, 1 (1985) 127.
29 A property of certain gels to become fluid when mechanically disturbed (as by shaking or stirring) then resetting after a period of time.
30 T. Bellini, M. Buscaglia, C. Chiccoli, F. Mantegazza, P. Pasini and C. Zannoni, Phys. Rev. Lett., 85 (2000) 1008.

Received: November 4, 2007
Accepted: January 11, 2008
OnlineFirst: June 26, 2008

DOI: 10.1007/s10973-007-8583-9